Journal of Energy Storage 26 (2019) 100976

Contents lists available at ScienceDirect

Journal of Energy Storage

journal homepage: www.elsevier.com/locate/est

Simulations and experimental validation of Pico conduit pressure hydropower systems with battery storage

L.N. Mbele, K. Kusakana*, S.P. Koko

Department of Electrical, Electronic and Computer Engineering Central University of Technology, Free State Bloemfontein, South Africa

ARTICLE INFO

Keywords:
Battery storage
Conduit Hydropower
Energy recovery
Excess pressure
Renewable energy

ABSTRACT

An increase in the world's population has led to an increased energy demand. Sustainable renewable energy sources must be broadly executed to fulfil the continuous need for energy. Amongst different renewable energy technologies, hydropower generation proved to be the most feasible solution. A portion of small hydropower can be acquired by recovering the energy inside water supply networks. This may lead to a sustainable electrification solution and reduced electricity bills for the water utility companies. Hence, the procedure of energy recovery using conduit hydro technology must be a part of the water cycle.

Numerous nations have started with the improvement of this innovative conduit hydro technology. However, very little has been exploited. Hence, this study focuses on developing a simulation tool that can be used to analyse conduit hydropower generation system with a battery storage. Subsequently, this paper exhibits the modelling and performance analysis of a small conduit hydropower system in MATLAB/Simulink software. This will assist the conduit hydropower developers to quantify the available energy and evaluate the viability of the conduit hydropower projects.

Furthermore, the performance of the modelled conduit hydropower system is compared to the performance of a prototype setup in a laboratory environment. Inlet water pressure was assessed to observe how the system reacts to the variation of the water pressure. This data was used to simulate the performance of the model in MATLAB/Simulink in comparison with the laboratory prototype. The results revealed that the developed model reacted viably under variable pressure. The conduit hydropower was just dynamic when the excess pressure was accessible, this is because of the pressure distinction between Pressure Reducing Valve (PRV) pre-set pressure and the system pressure. Hence, the excess pressure is used to drive the generator and the generated energy is then stored in the battery.

1. Introduction

Water supply networks' structures ought to adequately fulfil the water request prerequisites for local, business, and firefighting [1]. With respect to urban supply networks, the energy utilization in water supply networks peaks to 7% of the world's utilization of energy [2]. Water supply includes an energy footprint in the range of 0.18 and 0.32 kWh/m^3, as indicated by the California Energy Commission [3]. Energy investigation of these systems has demonstrated that an expansion of pressure is associated with expanded leakage [4].

In distribution networks, water is typically transported through pressurized channels, which might be set underground or over-the-ground [5]. The movement of water in these conduits relies upon the main force, which might be either pressure or gravity. The favoured main force in water conduit is gravity. The lack of gravity leads the pumping systems to push the water through a conduit.

Water conduits often have excess energy leading to high pressure or static head as well as high speed velocity rate. This may cause harm to the water supply network [6]. This has negative impacts, for example, resulting floods, prompting failure of the conduit system and fatigue failure of the pipeline, supports, instrumentation gear and components. This has prompted to a requirement for the integration of PRVs into system in order to dissipate excess energy and protect the system from harm [7]. However, PRVs do not optimize the accessible energy in the conduit. Instead, the excess potential energy of water is wasted.

PRVs decrease pressure and, therefore, the leakage volume. Hence, this necessitated the pioneering research to alternatives ways of recovering the energy dissipated by PRVs in water supply networks [8,9]. An eccentric arrangement was considered by replacing PRVs with a Pump as Turbines (PATs) [10].

* Corresponding author.
E-mail addresses: lmbele@cut.ac.za (L.N. Mbele), kkusakana@cut.ac.za (K. Kusakana), skoko@cut.ac.za (S.P. Koko).

https://doi.org/10.1016/j.est.2019.100976
Received 31 March 2019; Received in revised form 1 August 2019; Accepted 17 September 2019
2352-152X/

Nomenclature

ΣK_L	Secondary loss coefficient
B_m	Damping coefficient (N.m/s)
I	Current
i_d, i_q	d, q axis reference frame stator currents (A)
J_{eq}	Equivalent rotational inertia (kg.m^2)
J_g	Rotational inertia of the generator (kg.m^2)
J_{wt}	Rotational inertia of a water turbine (kg.m^2)
L_d, L_q	d, q axis reference frame inductances (H)
R_S	Stator resistance (ω)
v_d, v_q	d,q axis stator terminal voltages (V)
$\frac{fl}{2r_t}$	Main loss of coefficient caused by friction
€/Kw	Euro per kilowatt
cm	Centimetre
CO_2	Carbon dioxide
CO_2-e/kWh	Carbon dioxide emission per kilowatt hour
GW	Gigawatt
Hz	Hertz
km^3/year	Cubic kilometres per year
kPa	Kilopascal
Kw	Kilowatt
kWh	Kilowatt hour
kWh/m^3	Kilowatt hour per cubic meters
l/s	Litre per second
m	Meter
m^3/s	Cubic meter per second
mm	Millimetre
MW	Megawatt
N.m	Newton meter
N.m/s	Newton meter per second
N/m^2	Newton per square meter
Pa	Pascal
psi	Per square inch
rpm	Revolution per minute
Te	Electromagnetic torque of a generator (N.m)
Tm	Mechanical torque of a turbine rotor shaft (N.m)
W	Watt
??	Constant ranging from 0.6 to 0.65
f	Friction factor
l	Length of the bypass pipe
??	Mass of water
??	Radius of the main pipe
$??_{??}$	Radius of the bypass pipe
????	Radius of the PRV
$??_{??}$	Water velocity through the bypass pipe
??	Water density

Ferracota et al. [11] completed an examination on leakage reduction. They displayed and incorporated another specialized arrangement of replacing PRVs with PATs. The ideal working purpose of the PATs was chosen by utilizing a Variable Operating Strategy (VOS).

Carraveta et al. [12] built a PAT operating scheme with PRVs in parallel. This operating scheme and the variability of flows have encouraged studies on the development of VOS in these machines. These procedures permit the variety of the rotational speed of the pressure driven machine.

Ferracota et al. [13] have engaged studies to improve efficiency prospect in the machine through trial tests in semi-axial machines when the rotational speed differs. Preliminary studies in drinking water networks have been created through computational models.

Different studies have considered typical flows or hourly uniform examples in all utilization joints, for the improvement of water supply networks models [14,15]. These energy recuperation studies have advanced the utilization of water supply networks to produce clean energy by utilizing the dissipated energy in PRVs. These studies have brought some pilot establishments for evaluation purpose in different countries (e.g., Murcia (Spain), Portland (Oregon), Hong Kong, South Africa and Kildare (Ireland)).

The optimum use of energy is a key component in any conventional

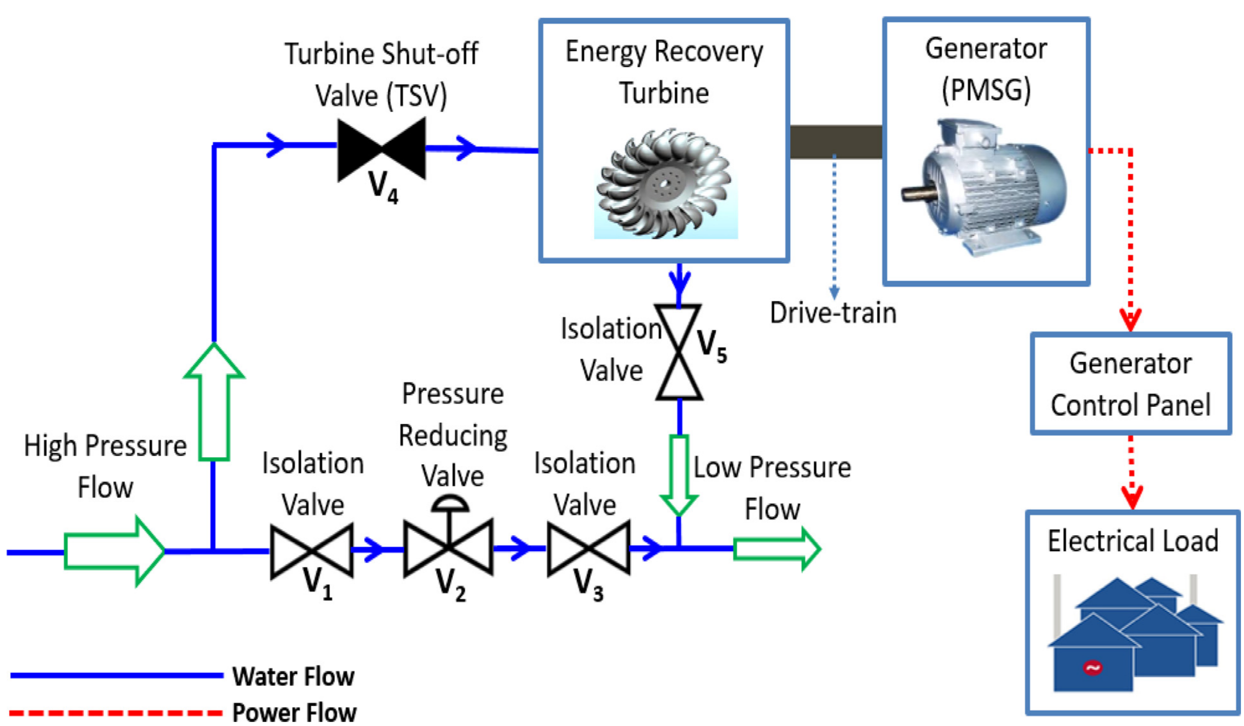

Fig. 1. Layout of a typical conduit hydropower generation system.

system, especially in the energy generation research field. In this manner, a parallel harvesting system might be utilized to convey excess water energy as opposed to permitting the dissipation through the PRVs. This is possible using a special kind of turbine and generator system to produce electricity by capturing the pressure head flow. This class of innovation is known as "Conduit hydropower" and is different from alternate classes of hydropower generation [16]. The excess energy accessible in pressurized water conduits is converted into clean and sustainable energy source. The conduit hydropower requires the least considerate work, since it uses the current water network without ecological effects [17]. For developing countries, such as South Africa, the application of this technology is new. Thus, four experimental plants were constructed, and the research project indicated that it is economically feasible and technically possible to generate electricity from water supply systems, as discussed in the technical papers [18,19].

It may be concluded that in the literature available today, none of the studies presented/proposed a simulation tool that can be utilized to analyse the performance of the conduit Pico hydropower system. Therefore, in this work, a model of conduit hydropower is developed and simulated in MATLAB/Simulink. This model aims to show the generated outputs power parameters and can be used to analyse the dynamic performance of the system for different sites and varying operational conditions. To perform the experimental trial tests, a small conduit hydropower model is set-up in order to quantify the electrical parameters as to verify the simulation results.

2. Model development for small conduit hydropower generation system

In this section, a scientific model is developed for analysing the behaviour of the proposed energy recovery system. The primary components of the system to be modelled incorporate the energy recovery turbine, drive-train and the generator. The component size and simulation parameters are additionally introduced.

2.1. System description

With an end-goal to harness the power from high pressured water that flows through water supply networks consistently, an ever-increasing number of nations are investigating the likelihood of conduit hydropower innovation. Fig. 1 demonstrates the general layout of the conduit hydropower system. In conduit hydropower generation, small energy recovery turbines or PATs are introduced in water supply network where dissipation of pressure is essential. The pressure is ordinarily dissipated using PRVs which dissipate the energy related with the flow over the pressure differential. The introduced turbines or PATs intend to recover a part of the energy and convert it into useable energy that can be utilized to supply the loads.

The conduit hydropower system is placed parallel to another or existing PRV depicted as V2 in Fig. 1. This parallel valve turns into the turbine bypass valve. During the absence of excess pressure, the water will flow regularly through the essential conduits by means of V1, V2 and V3. At the point when excess pressure is accessible from the high-pressure side, the excess energy recovery starts from the bypass/secondary conduit, opening Turbine Shut-off Valve (TSV) (V4) to permit flow through a turbine down towards V5 and out to the low-pressure side. At the point when the turbine is down for maintenance, water can still be transported to consumers without any interference. A programmed safeguard valve TSV (or V4) is introduced on the high-pressure side of the turbine works as a turbine shut-off valve. This valve enables the prime-mover path to be securely closed in case of power cuts or crisis circumstance. The turbine control system naturally exchanges water flow from the turbine to the bypass control valve and back upon start up and shut down.

2.2. Turbine model

Water energy is exceptionally fast inside water supply networks. The water kinetic energy E is extracted for a specific period/time t through the utilization of a hydro turbine with efficiency η. In this manner, the mechanical power created by the hydro turbine can be expressed as follows [20]:

$$P = \frac{E}{t} \times \eta \tag{1}$$

$$E = \frac{1}{2} m v_t^2, \ \ m = \rho \pi r_t^2 t \tag{2}$$

Where:

m = water mass (kg);
ρ = density of water (1000 kg/m^3);
v_t = velocity of water in the bypass pipe (m/s);
r_t = bypass pipe radius (m).

Substituting Eq. (2) into (1) the power created by the water turbine can be expressed by [21]:

$$Pm = \frac{\rho \pi r_t^2 v_t^3}{2} \times \eta \tag{3}$$

The turbine is installed directly into the bypass pipe as shown in Fig. 1. The decision of this design is encouraged by a decision of limiting the disturbances in the main supply cycles.

This system is designed such that the water turbine is driven by the change in water pressure after the PRV. The pressure distinction, at the bypass inlet and outlet respectively, is reliant on the flow rate (??) and is expressed as follows [21]:

$$p_1 - p_2 = \frac{Q^2 \rho}{2\pi^2 r_v^4 c^2}\left[1 - \left(\frac{r_v}{r}\right)^4\right] \tag{4}$$

Where:

$P_1 - P_2$ = the pressure difference between the main pipe (P_1) and the bypass pipe (P_2);
Q = the water flow rate (m^3/s);
?? = the constant ranging from 0.6 and 0.65;
???? = the radius of the PRV (m);
?? = the radius of the main pipe (m).

To produce the mechanical energy (*Pm*) from the previous Eq. (3), mechanical power needs to be converted into torque, thereby dividing it by the angular speed of the rotating shaft (*Wm*), toque must be multiplied by (−1) to be in generator mode. Additionally, water speed should be definite considering a turbine driven by the pressure drop at PRV. The water speed in the bypass pipe is given by the Eq. (5) below [21]. This considers all the losses in the bypass pipe, for example, main loss coefficient that is brought about by the friction of the straight section of the bypass pipe as well as the auxiliary loss coefficient that is brought about by different parts of the bypass pipe such the entrance at the inlet point 1, elbows of the bending sections, and the exit at the outlet point 2.

$$v_t = \sqrt{\frac{2(p_1 - p_2)}{\rho\left(\frac{fl}{2r_t} + \sum K_L\right)}} \tag{5}$$

Where:

$\frac{fl}{2r_t}$ = main loss of coefficient caused by friction,
f = friction factor,
l = length of the bypass pipe,
ΣK_L = secondary loss coefficient of other components in the bypass

pipe.

The losses caused by the turbine is neglected in Eq. (5) because it is already considered in the efficiency of the turbine. The developed Simulink model of the energy recovery turbine is as shown in Fig. 2.

2.3. Drive train model

The drive train enables the transformation of kinetic energy of water flowing in the energy recovery system into useful mechanical energy. The drive train can be in a form of gears or directly driven. On the off chance that gears are utilized in the shaft, the gearbox inside the drive train interfaces the low-speed shaft (on the water turbine side) with the fast shaft associated on the rapid shaft (on the PMSG side). This coupling gives high rotational speed required by the generator to create power to a specific level.

However, the utilization of this coupling can expand project costs, decrease the unwavering quality and effectiveness of the system. This is due to the energy losses and regular maintenance required to keep the system running [21]. Subsequently, a direct coupling is ideally an efficient technique.

The drive train can be modelled utilizing distinctive strategies, for example, one-mass, two-mass or three-mass [21]. Since the point of this research is to recuperate energy from excess pressure and create electrical yield energy, the drive train was treated as one-mass.

This implies that all inertia components are modelled as a one rotary mass or direct coupling. This coupling takes into consideration the mechanical torque from the water turbine $T_{w:g}$ to be proportional to the mechanical torque of the generator T_m. Additionally, the rotor angular speed of the turbine ω_g is equivalent to the rotor angular speed of the generator ω_m. The relationship is then given by the Eqs. (6) and (7), respectively [21].

$$T_{w:g} = T_m \tag{6}$$

$$\omega_g = \omega_m \tag{7}$$

The mechanical torque from the turbine to the generator enables the generator to deliver electromagnetic torque T_e which is represented as follows [21]:

$$T_e = J_{eq} \times \frac{d\omega_g}{dt} + B_m \times \omega_g + T_{W:g} \tag{8}$$

Where:

B_m = damping coefficient (Nm/s);
J_{eq} = equivalent rotational inertia of a generator and turbine (kg.m^2), which is determined using Eq. (9) as follows [21]:

$$J_{eq} = J_g + J_{wt} \tag{9}$$

Where:
J_g = rotational inertia of the generator (kg.m^2);
J_{wt} = rotational inertia of a water turbine (kg.m^2).

The benefit of utilizing PMSG is that they are low inertia machines since J_g is irrelevantly small making J_{eq} practically identical to J_{wt}. Fig. 3 shows a MATLAB/Simulink block diagram for a one-mass drive train or a direct drive coupling, through the following assumptions:

The turbine inertia (5 kg.m^2) was utilized as J_{eq}.

Rotational damping coefficient was assumed to be equal to zero.

From Eq. (8), the angular speed of the generator shaft ($\frac{d\omega_g}{dt}$) can be expressed as indicated by Eq. (10) below [21]:

$$\frac{d\omega_g}{dt} = \frac{T_e - T_{w:g}}{J_{eq}} - \frac{B_m}{J_{eq}} \times \omega_g \tag{10}$$

The angular acceleration ω_g is an input energy to the PMSG. This energy is changed over to electrical angular speed ω_e of the generator.

2.4. Generator model

The Permanent Magnet Synchronous Generator (PMSG) model can be developed by representing the rotor with three windings: one being the field and the other two being the D-and q-axis "damper" windings, representing the effects of the rotor and other current conveying paths [22]. The damping effect is thought to be insignificant (of both the rotor and magnets), the flux circulation in the rotor is sinusoidal, unsaturated magnetic circuit, insignificant iron losses and the absence of field current dynamics. It should be noted all the presumed computations and data presented in this section are very important in providing insight into operational parameters.

An appropriate transformation may be applied to the stator variable, in order to study the response of PMSG. To begin, assume that the PMSG can be appropriately represented by five equivalent windings. Three of these windings, the armature phase windings and the other two, representing the effects of distributed currents on the rotor, further known as the "damper" windings. Park Transformation is mostly used for modelling three phase machines. It transforms the parameters and equation from the stationary form into direct-quadrature (d-q) axis. It converts three phase quantities to direct current quantities, ABC to d-q transformation. The dynamic model of the generator is developed from two-stage reference frame, in which the q-axis is 90° ahead of the d-axis with respect to rotational direction. The connection between the electrical angular speed and rotor angular speed of the generator is represented by Eq. (11) considering the electrical angle (θ_e) between the stator phase A axis and the d-axis [21].

$$\frac{d\theta_e}{dt} = p \times \omega_g = \omega_e \tag{11}$$

At the point when the rotor position is known, Park's transformation can be applied to compute the direct axis, quadrature-axis and zero sequence values in a two rotary reference frame for a three phase sinewave signal. These parts can be controlled to impact the active and reactive power, respectively.

Assuming that the flow direction of the negative stator current is out of the generator's positive polarity terminals, the d-q reference stator voltages can be represented to by Eqs. (12) and (13) separately [21,22]:

$$v_d = R_s i_d + L_d \frac{di_d}{dt} - \omega_e L_q i_q \tag{12}$$

$$v_q = R_s i_q + L_q \frac{di_q}{dt} - \omega_e \psi_{pm} + \omega_e L_d i_d \tag{13}$$

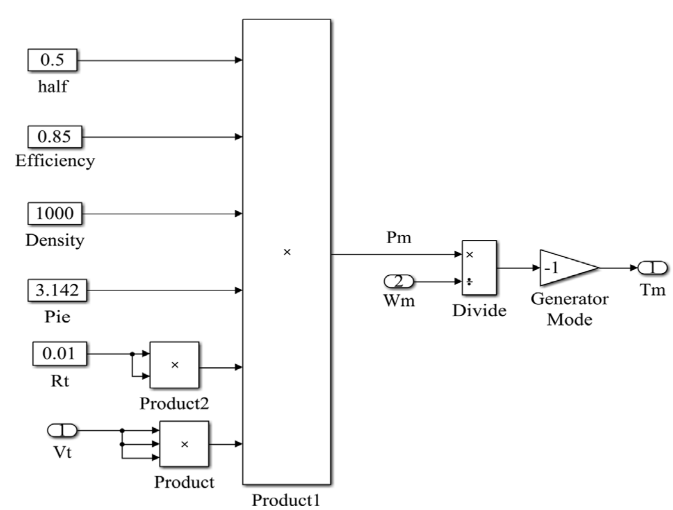

Fig. 2. Simulink model for the energy recovery turbine.

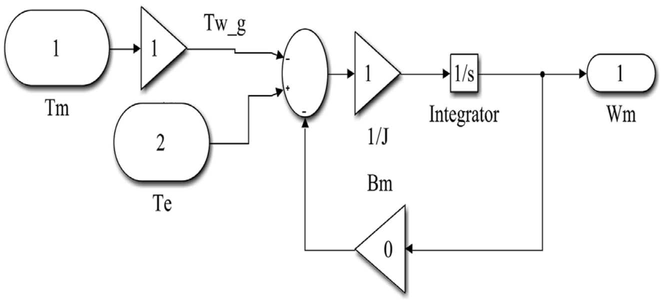

Fig. 3. Simulink model for the drive train.

Where:

v_d and v_q = the stator terminal voltages in the d-q axis reference frame (V);
R_S = the stator resistance (Ω);
L_d and L_q = the d, q axis reference frame inductances (H);
i_d and i_q = the d, q axis reference frame stator currents (A);

Eqs. (12) and (13) can be simplified to obtain the output d and q currents of the generator as represented by Eqs. (14) and (15) [21,22].

$$i_d = \int\left(\frac{v_d}{L_d} - \frac{R_s}{L_d}i_d + \frac{L_q}{L_d}\omega_e i_q\right)dt \tag{14}$$

$$i_q = \int\left(\frac{v_q}{L_q} - \frac{R_s}{L_q}i_q + \frac{L_d}{L_q}\omega_e i_d - \frac{\psi_{pm}}{L_q}\omega_e\right)dt \tag{15}$$

In the rotor frame, the created electromagnetic torque is reliant upon the cross-result of stator flux and stator current, the expression is given by Eq. (16) below.

$$T_e = \frac{3}{2}(\psi_{pm} i_q + (L_d - L_q)i_d i_q) \tag{16}$$

The transformation for three phase voltage elements (Vabc) into DC voltage elements (Vd-q) is represented by Eq. (17), ignoring the zero-phase sequence in order to simplify the transformation [9–11].

$$\begin{pmatrix} v_d \\ v_q \end{pmatrix} = \frac{2}{3}\begin{pmatrix} \cos\theta_e & \cos\left(\theta_e - \frac{2\pi}{3}\right) & \cos\left(\theta_e + \frac{2\pi}{3}\right) \\ \sin\theta_e & \sin\left(\theta_e - \frac{2\pi}{3}\right) & \sin\left(\theta_e + \frac{2\pi}{3}\right) \end{pmatrix}\begin{pmatrix} V_a \\ V_b \\ V_c \end{pmatrix} \tag{17}$$

The transformation for the relating Three phase currents is acquired through reverse transformation of the DC currents (Id-q), ignoring the zero phase sequence current (I_0). The three phase currents are then represented by Eq. (18) below [21,22]. The final Simulink block of the generator is represented as shown in Fig. 4.

$$\begin{pmatrix} i_a \\ i_b \\ i_c \end{pmatrix} = \frac{2}{3}\begin{pmatrix} \cos\theta_e & \sin\theta_e \\ \cos\left(\theta_e - \frac{2\pi}{3}\right) & \sin\left(\theta_e - \frac{2\pi}{3}\right) \\ \cos\left(\theta_e + \frac{2\pi}{3}\right) & \sin\left(\theta_e + \frac{2\pi}{3}\right) \end{pmatrix}\begin{pmatrix} i_d \\ i_q \end{pmatrix} \tag{18}$$

2.5. Complete Simulink block diagram of the conduit hydropower generation system

The final energy recovery system is represented as shown in Fig. 5 below. This block comprises of various components of the system are connected together. Each block contains a sub system, through which all the algorithms were modelled.

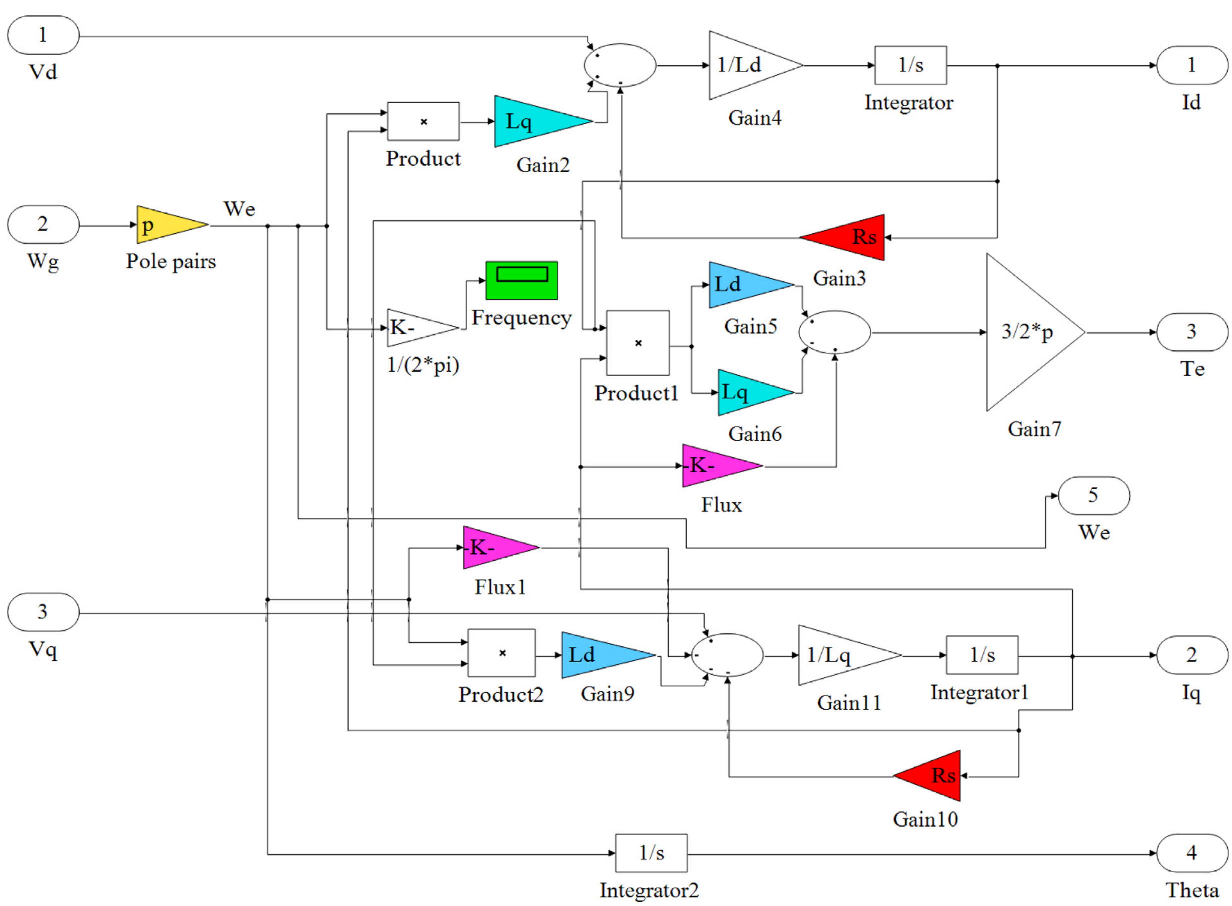

Fig. 4. Simulink model of the generator.

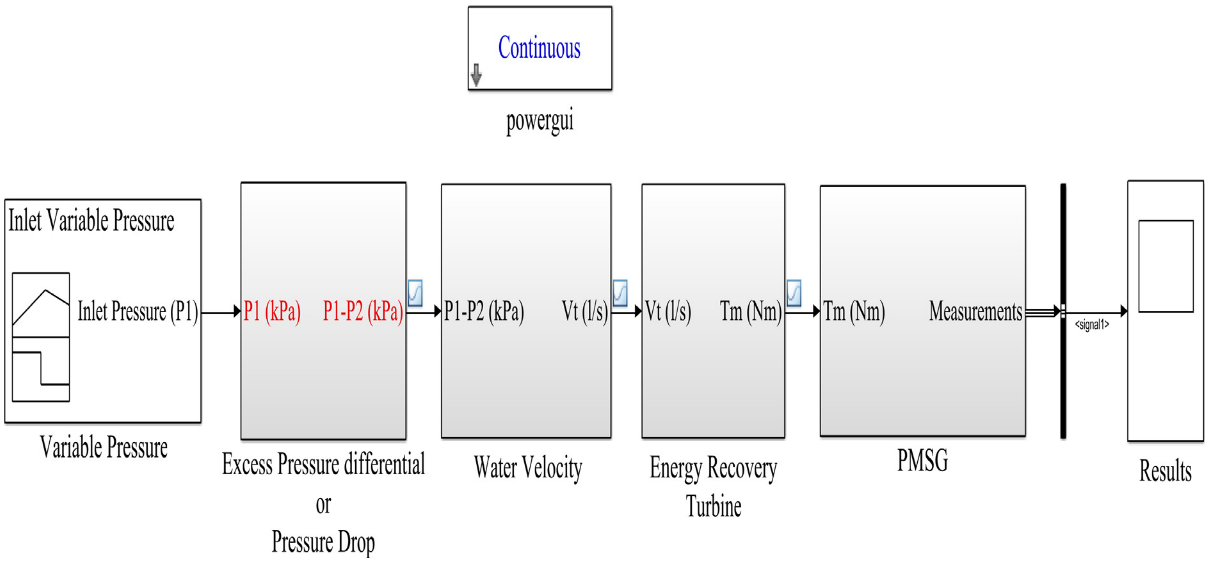

Fig. 5. Final Block Model for Conduit hydropower generation.

Table 1
Simulation parameters.

Component	Parameters	
Conduit Bypass pipe	Friction coefficient	0.02
	Length	1 m
	Radius	4.8 cm
	Entrance losses	0.35
	Elbow losses	1.7
	Exit losses	1
Turbine	Efficiency	85%
PMSG (Salient pole)	Ld	0.02547
	Lq	0.02816
	Rs	2 ohms
	Pole pairs	3
Load	Nominal Power	1 kW
	Frequency	50 Hz

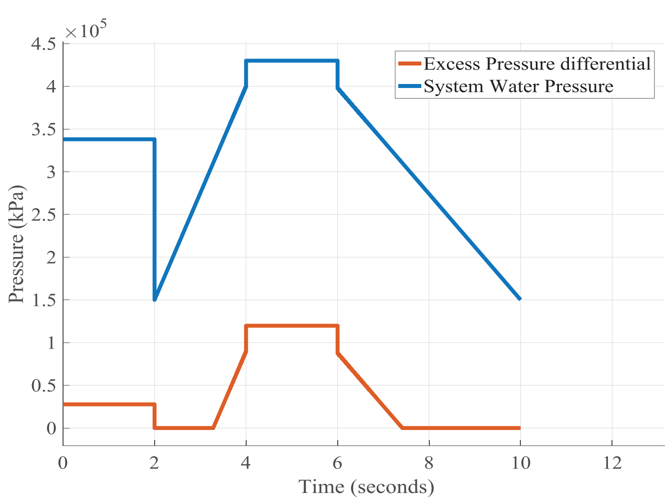

Fig. 6. Presssure comparison for 10 s.

2.6. Simulation parameters

The size and parameters identified with the three significant components of the conduit hydropower generation system are recorded in Table 1 [23].

3. Model simulation results

To study the dynamic reaction of the conduit hydropower generation system under inconstant pressure, the step input that represent excess pressure has been utilized entirely for simulation purpose. The execution results are shown in Figs. 6–10. The system pressure was 340 kPa for the initial 2 s while the abundance weight was 40 kPa. The system water pressure achieved 150 kPa following 2 s and achieved a limit of 430 kPa following 4 s. The accessible excess pressure followed the equivalent graphical pattern given by the system pressure. After 2 s the excess pressure was least at zero then achieved a limit of 119 kPa for the following 4 s at as shown in Fig. 6.

The water velocity is specifically relative to the accessible excess pressure in the system. When the water velocity is zero, the excess pressure is zero. Between 4 and 6 s, the water velocity reached the maximum value of 8573 l/s due to an increased excess pressure, as shown in Fig. 7.

The mechanical torque of the energy recovery system is inversely relative to the accessible excess pressure. As excess pressure achieved its minimum, the mechanical torque was at zero following 2 s. As the excess pressure achieved its maximum, the mechanical torque achieved a maximum value of -0.3139 Nm, as shown in Fig. 8.

The produced three-phase voltages and currents is reliant on the accessible excess pressure. The system voltages and currents were at minimum from 0 to 4 s. Due to large amount of excess pressure, the system voltages and currents are at maximum from 4 to 6 s period, as shown in Fig. 9.

The electromagnetic torque of the PMSG is directly relative to the mechanical torque of the turbine, this shown in Fig. 10. It was expected that both electrical and mechanical torques follow a similar trend, knowing that both generator and turbine shafts were directly connected. The negative torque values represent the rotation of the shaft and the 0 torque values represent no rotation of the shaft. This trend was dependant upon excess pressure recovery.

From the simulation results obtained in Figs. 6–10, it is evident that the model performance is in line with the objectives of this research. Hence, Further verification using experimental prototype results is required to validate the model.

4. Experimental analysis

In this section the results of the experiments conducted on the laboratory prototype are analysed. The aim is to validate the effectiveness

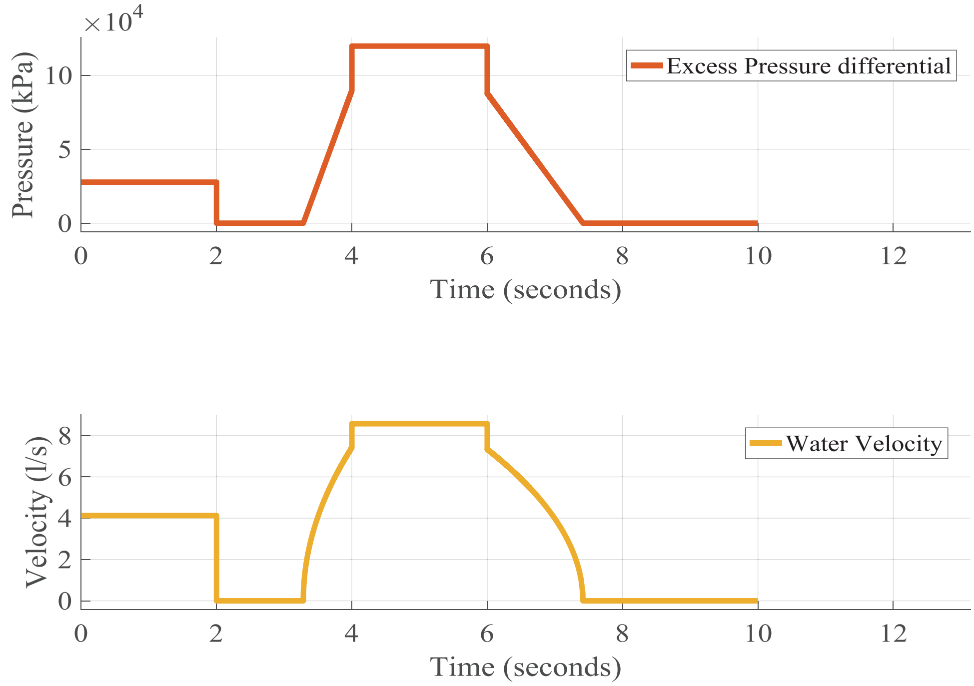

Fig. 7. Excess Pressure as compared to Water Velocity for 10 s.

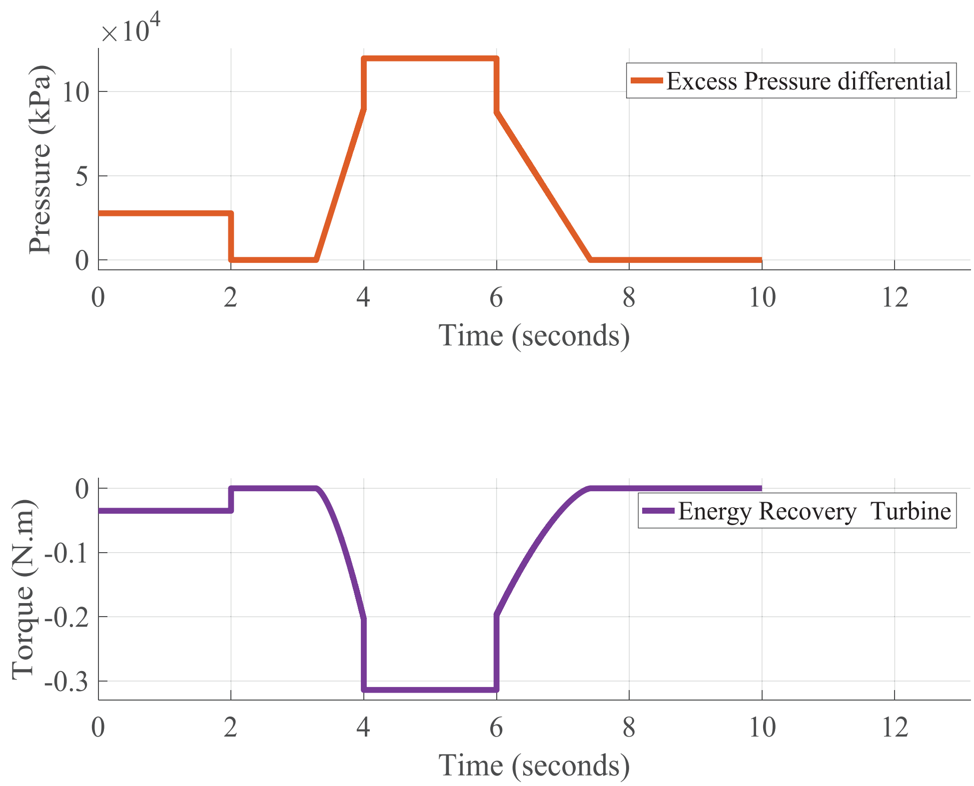

Fig. 8. Excess Pressure Differential as compared to Mechanical Torque for 10 s.

of the developed model. Although the generator used for the practical experiments is different from the one used for simulation in Section 3, this does not have significant negative implications on the contribution of the study. For experimental analysis, a Brushless Permanent Magnet DC Generator (BPMDCG) was used. The objective is to experiment or interpret the effectiveness of the developed model. This is done by studying the dynamic behaviour of a conduit hydropower generation system under inconstant water pressure.

The performance of the modelled conduit hydropower system is thus compared to the performance of a laboratory prototype. Inlet water pressure was measured to analyse how the system reacts to a change in water pressure. This data is used to simulate the performance of the model in MATLAB/Simulink in comparison with the experimental results.

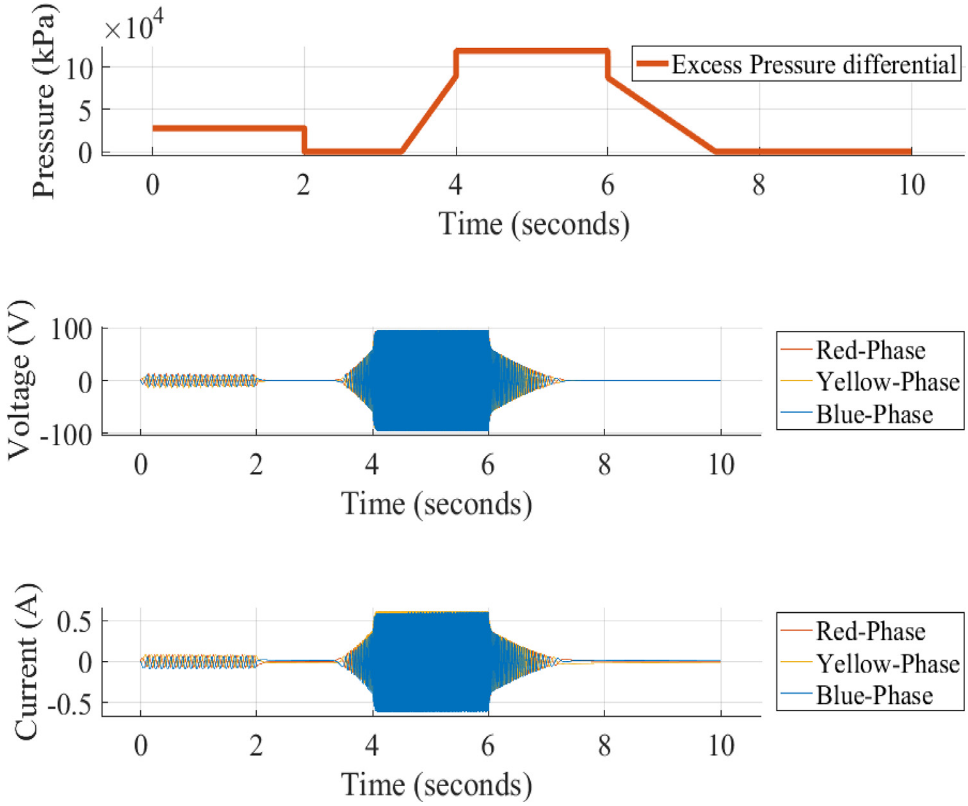

Fig. 9. Voltage and Current Relative to Excess Pressure for 10 s.

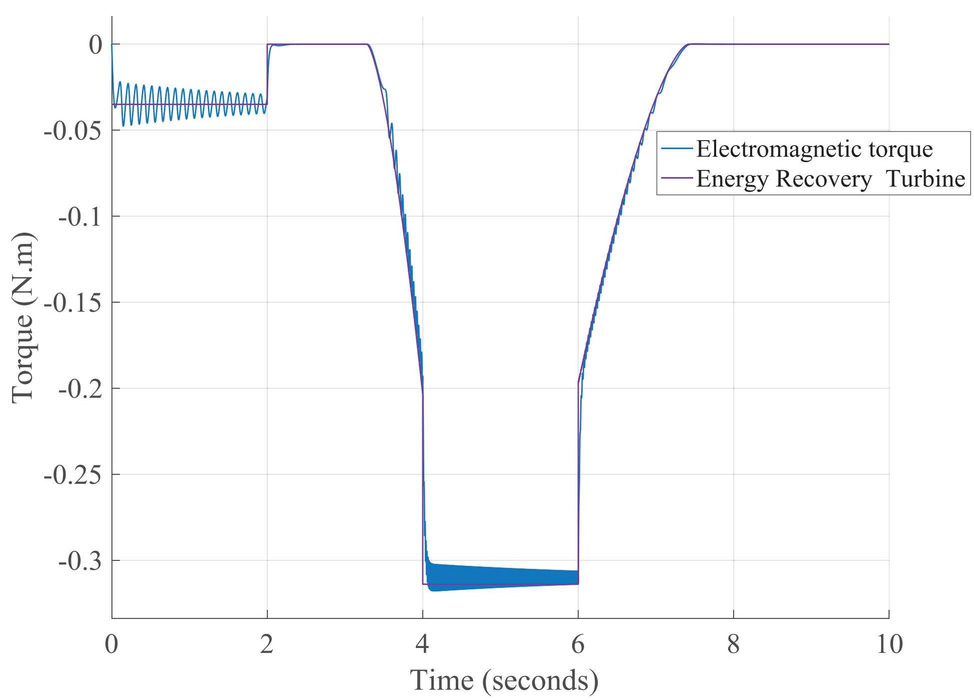

Fig. 10. Electromagnetic Torque Vs Mechanical Torque.

Table 2
Electrical parameters.

Rated output voltage	12 VDC
Maximum output current	2.2 A
Rated output power	25 W
Type of batteries allowed	Sealed lead-acid according to EN60896-11:2003
Battery capacity	[9-45] Ah

4.1. Practical setup description

The laboratory set-up of the conduit hydropower generation system is designed in such a way to generate electric energy from a circulating water flow and a pressure differential. The electrical energy is generated using a Brushless Permanent Magnet DC Generator (BPMDCG). The generated energy is stored in a battery, to which various loads can

Table 3
Hydraulic parameters.

Maximum pressure at the entrance P1_max	10 bar
ΔMinimum entry-exit operating pressure	0.45 bar
ΔMaximum entry-exit working pressure	1.8 bar
ΔAbsolute maximum input-output pressure ΔPmax	2.0 bar
Minimum operating flow	0.5 L/s
Maximum working flow	0.95 L/s
Absolute maximum flow Qmax	1.0 L/s

be connected and whose energy consumption must always be lower than the energy produced by the system.

The system has an aligned input and output hydraulic design and a defined flow direction. The hydraulic body and electric generator form a single compact unit without the need for a mechanical closure. The electrical and hydraulic parameters of the system are as shown in Tables 2 and 3, respectively. The complete installation of the conduit hydropower generation system is as shown in Fig. 11 below.

4.2. Experimental results

For experimental characterisation, the BPMDCG was linked with a local water pipe line (3 bar static weight). In this set-up, the flow rate can be altered between 0.69 l/s and 3 l/s. These values were measured on the inlet pipe of the proposed system. This flow metre could not be shown in the picture because a close up photo was chosen to display all important parts of the proposed system. The voltage and current yields have been measured over a 1-ohm load resistor. A rechargeable 12 V battery was connected to the generator, as per manufacture's manual. The generator cannot operate without the battery. During voltage and current measurements, the initial circuit voltage/start-up voltage was considered for accuracy of the results. The difference in the measured

Table 4
Experimental results.

Water flow (l/s)	Inlet pressure (kPa)	Outlet pressures (kPa)	Pressure drop (kPa)	Voltage difference (ΔV)	Charging current (A)
0,69	40	0	40	0	0
0,89	50	5	45	0	0
1089	110	6	104	0.06	0,2
1277	150	25	125	0.83	0,9
1,5	200	35	165	1.94	1,2
1,7	260	40	220	1.94	1,2
1,93	340	40	300	1.94	1,23
2,2	440	43	397	1.94	1,23

and the start-up voltage is equal to the actual voltage generated. The pressure drop of the energy recovery system was also calculated. The measured data is summarized in Table 4. This data was then used to plot graphic representation of the prototype results in order to compare with the MATLAB/Simulink model results.

Table 4 shows the experimental prototype results for the BPMDCG. From Table 4 above, the inlet pressure data was imported to MATLAB for computing a graphical data plot as shown Fig. 12 below. This data was also used as input to the developed conduit hydropower generation model. When the water flow is below 1 l/s, the inlet pressure goes below 100 kPa. This is because the turbine embedded directly in the BPMDCG utilizes most of the inlet pressure to drive the generator; hence resulting to a significant drop of the outlet pressure. The amount of the utilized pressure is indicated by the pressure drop. An increase in pressure drop leads to the rise in voltage difference (ΔV). The charging currents is significantly low during the initial start-up of the BPMDCG and is expected to rise relative to an increase in water flow. The safety feature of the BPMDCG is to charge the battery up to a saturation point

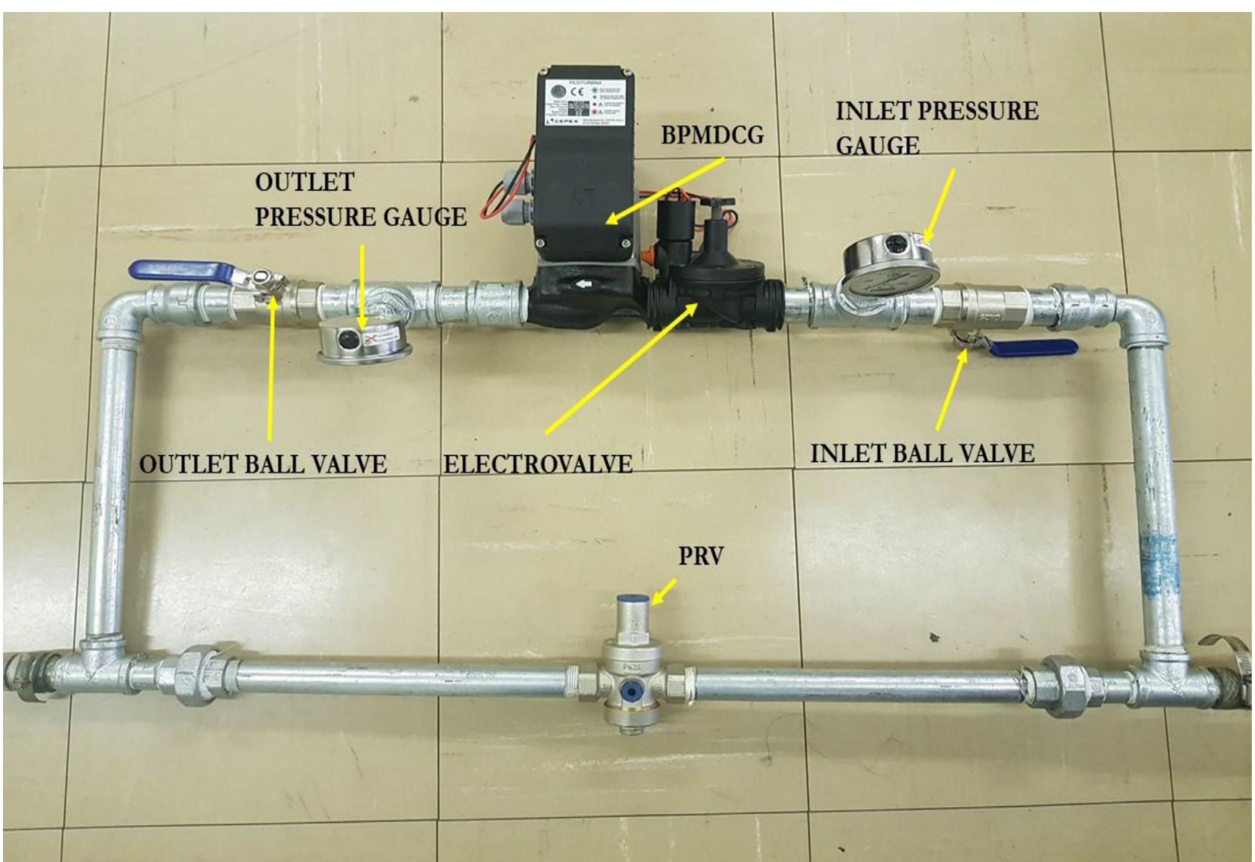

Fig. 11. Laboratory set-up Conduit Hydropower Generation System.

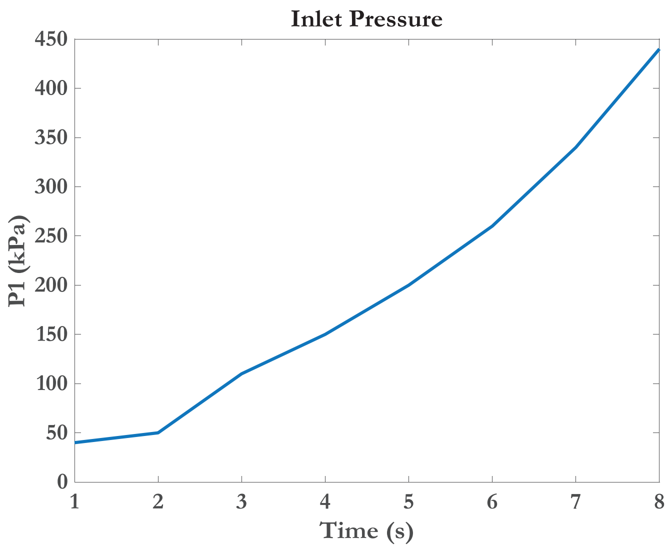

Fig. 12. Inlet Pressure data.

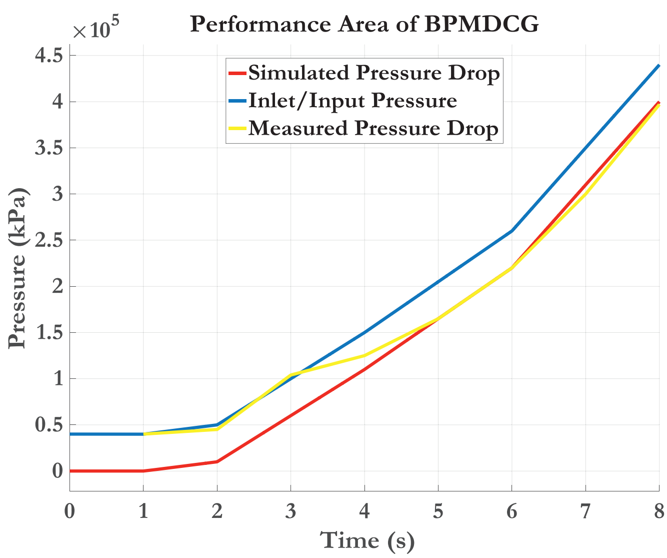

Fig. 13. Performance area of BPMDCG.

of 13.94 V, thereby resulting in the voltage difference of 1.94 V (ΔV) during saturation.

The inlet pressure varied from 40 kPa to 440 kPa as indicated in Fig. 12. This is normal as there is variable water demand in the municipal water supply systems. Pressure fluctuates relative to the varying water demand. Less demand leads to an increased pressure and more demand leads to a reduces pressure in the system. Therefore, pressure fluctuation opens a door for possible excess pressure recovery as indicated in Fig. 13.

In Fig. 13 above, inlet pressure forms basis for comparison of the measured pressure drop versus the simulated pressure drop. The comparison is done in order to analyse the performance or operating area of the conduit hydropower generation system. In the first 5 s, there is Significant variation between the measured and the simulated pressure drop. The simulation model has a greater operating area than the prototype. After 5 s both graphs revealed almost identical pressure drops. This implies that the both systems utilises/extracts almost the same amount of pressure needed for conduit hydropower generation.

The generated voltages (ΔV above the battery voltage) of the measured and the simulated data are shown as shown in Fig. 14. It can be noticed that the measured voltage is less than the simulated voltage.

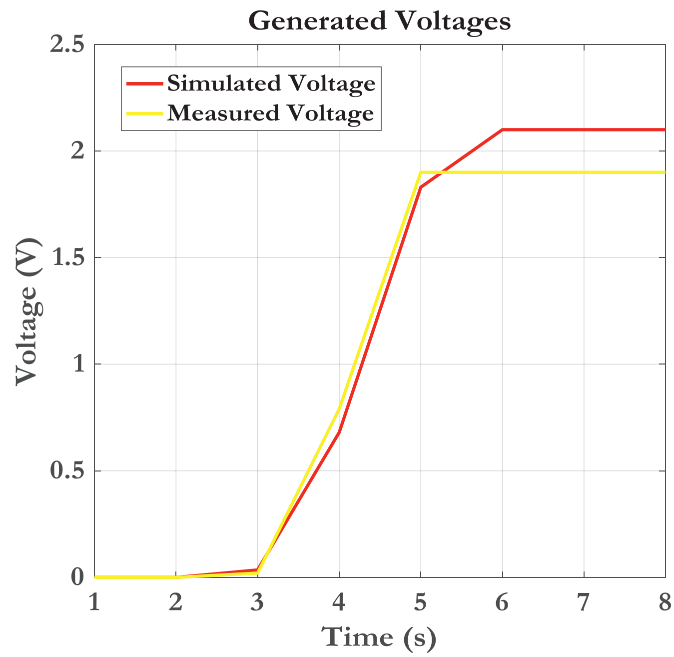

Fig. 14. Generated Voltages (ΔV).

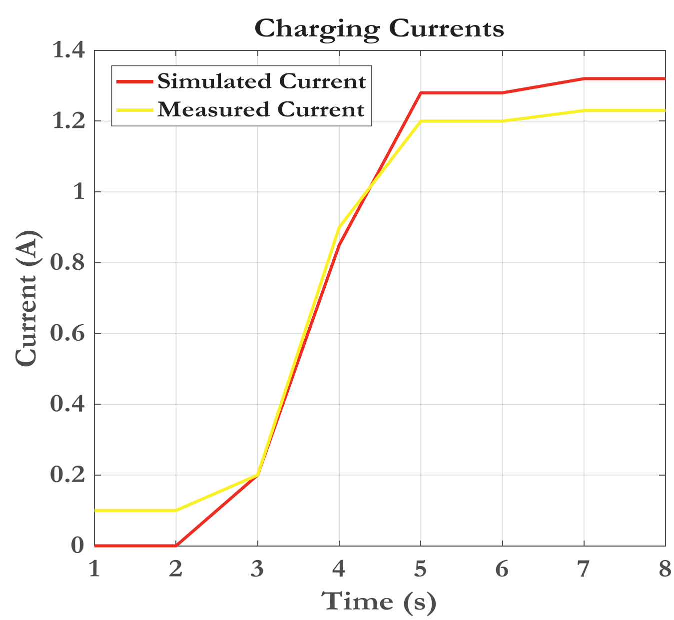

Fig. 15. Charging Currents.

This is due to the operating area of the actual prototype being smaller than the one of the developed model. The prototype can reach saturation at around 1.94 V, which above the battery rating. The reason is to prevent damage on the generator during charging of the battery. The saturation voltage is equal to the contrast between the initial start-up voltage and the maximum output voltage of the BPMDCG. For the same reason, one can expect the same relationship between the charging currents as shown in Fig. 15 below.

5. Conclusion

This paper exhibited the mathematical modelling of a small conduit hydropower system utilizing MATLAB/Simulink software. The performance of the modelled conduit hydropower system was compared to the performance of a prototype system, in order to validate the developed model. The findings revealed that the created model reacted successfully under dynamic pressure condition. The system was just dynamic when the excess pressure was accessible, this is because of the pressure distinction between PRV pre-set weight and the system pressure. At the point when the system pressure was more prominent than the pressure setting at PRV, the energy recovery turbine used the pressure distinction to drive the PMSG. Typical voltages and currents were achieved, and the results revealed that when the pressure drops to zero, the generator is unable to produce electricity.

The created model can be utilized by engineers to study the system performance under dynamic weight. Since there is correlation between an increase in excess pressure and the generated output power, it is imperative to limit the energy recovered by the turbine in order to safeguard the generator life span.

For future work, further research is required to address factors not covered by this work. This may include the assessment of various turbines and generators innovations as well as the whole efficiency of the energy recovery process. Additionally, the performance of the model needs to be assessed under various setup of the pipeline framework as well as the exhaustive examination of the physical misfortunes in the pipeline.

References

[1] L. Mbele, K. Kusakana, Overview of conduit hydropower in South Africa: status and applications, Power Africa, 2017 IEEE PES, IEEE, 2017, pp. 385–390.
[2] B. Coelho, A. Andrade-Campos, Efficiency achievement in water supply systems—A review, Renew. Sustain. Energy Rev 30 (2014) 59–84.
[3] G. Klein, M. Krebs, V. Hall, T. O'Brien, B.B. Blevins, California's Water–Energy Relationship, California Energy Commission, 2005.
[4] E. Cabrera, M.A. Pardo, R. Cobacho, E. Cabrera Jr., Energy audit of water networks, J. Water Res. Plan. Manag. 136 (6) (2010) 669–677.
[5] M. Casini, Harvesting energy from in-pipe hydro systems at urban and building scale, Int. J. Smart Grid Clean. Energy 4 (2015) 316–327.
[6] C.J. Hős, A.R. Champneys, K. Paul, M. McNeely, Dynamic behaviour of direct spring loaded pressure relief valves connected to inlet piping: iv review and recommendations, J. Loss Prev. Process. Ind. 48 (2017) 270–288.
[7] M. Sinagra, V. Sammartano, G. Morreale, T. Tucciarelli, A new device for pressure control and energy recovery in water distribution networks, Water 9 (5) (2017) 309.
[8] H. Ramos, A. Borga, Pumps as turbines: an unconventional solution to energy production, Urban Water 1 (3) (1999) 261–263.
[9] A. Carravetta, G.D. Giudice, O. Fecarotta, H.M. Ramos, Energy production in water distribution networks: a PAT design strategy, Water Res. Manag. 26 (13) (2012) 3947–3959.
[10] A. Carravetta, G.D. Giudice, O. Fecarotta, H.M. Ramos, PAT design strategy for energy recovery in water distribution networks by electrical regulation, Energies 6 (1) (2013) 411–424.
[11] O. Fecarotta, C. Aricò, A. Carravetta, R. Martino, H.M. Ramos, Hydropower potential in water distribution networks: pressure control by PATs, Water Res. Manag. 29 (3) (2015) 699–714.
[12] A. Carravetta, S.D. Houreh, H.M. Ramos, Pumps as turbines: Fundamentals and Applications, Springer, 2017.
[13] O. Fecarotta, A. Carravetta, H.M. Ramos, R. Martino, An improved affinity model to enhance variable operating strategy for pumps used as turbines, J. Hydr. Res. 54 (3) (2016) 332–341.
[14] M. Pérez-Sánchez, F.J. Sánchez-Romero, H.M. Ramos, P. Amparo López-Jiménez, Energy recovery in existing water networks: towards greater sustainability, Water 9 (2) (2017) 97.
[15] B. Lisk, E. Greenberg, F. Bloetscher, Implementing Renewable Energy at Water Utilities; Case Studies, Water Research Foundation, Denver, CO, USA, 2012.
[16] K. Kusakana, A survey of innovative technologies increasing the viability of micro-hydropower as a cost effective rural electrification option in South Africa, Renew. Sustain. Energy Rev. 37 (2014) 370–379.
[17] I. Loots, M.V. Dijk, B. Barta, S.J. Van Vuuren, J.N. Bhagwan, A review of low head hydropower technologies and applications in a south african context, Renew. Sustain. Energy Rev. 50 (2015) 1254–1268.
[18] I. Loots, M.V. Dijk, S.J. Van Vuuren, J.N. Bhagwan, A. Kurtz, Conduit-hydropower potential in the city of Tshwane water distribution system: a discussion of potential applications, financial and other benefits, J. S. Afr. Instit. Civi. Eng. 56 (3) (2014) 02–13.
[19] M.V. Dijk, Conduit hydropower: an alternative sustainable renewable energy source. Conduit hydropower an Altern, Sustain. Renew. Energy Source 9 (2014) 27–31.
[20] K. Kusakana, A survey of innovative technologies increasing the viability of micro-hydropower as a cost effective rural electrification option in South Africa, Renew. Sustain. Energy Rev. 37 (2014) 370–379.
[21] S.P. Koko, K. Kusakana, H.J. Vermaak, Micro-hydrokinetic river system modelling and analysis as compared to wind system for remote rural electrification, Electr. Power Syst. Res. 126 (2015) 38–44.
[22] L. Mbele, K. Kusakana, Modelling water energy recovery system using MATLAB/Simulink software, Adv. Sci. Lett. 24 (11) (2018) 8209–8214.
[23] L.N. Mbele, K. Kusakana, Model-based design of a conduit Pico hydropower system, 2018 IEEE PES/IAS Power Africa, IEEE, 2018, pp. 769–774.